Earth, Planets and Space

EXPRESS LETTER

Open Access

Testing determinations of Thellier paleointensities on 1962 and 1983 lava flows and scoriae in Miyakejima, Japan

Koji Fukuma*

Abstract

Using a fully automated magnetometer, test measurements of paleointensity by the Thellier method were performed on basaltic lava sections, including upper and lower clinkers through the lava interior, and scoriae that erupted from Miyakejima Volcano in 1962 and 1983. Curie temperatures showed a bimodal distribution with titanium-rich and -poor titanomagnetites, and in many cases two phases coexisted in a single sample. Thermomagnetic analyses on all samples prior to the Thellier measurements helped set appropriate temperature steps during Thellier measurements for individual samples. The Thellier results were selected using a combination of TTA and curvature criteria to detect thermal alteration and multidomain effects. Two-thirds of the clinker and scoria samples passed the criteria, which is 4.3 times higher compared to the lava interior. Paleointensities at all six sites are not largely different from the expected geomagnetic field intensities, and the averaged paleointensities for the 1962 and 1983 lavas/scoriae are within 5% of the expected intensities. Pass and fail samples have distinctly different hysteresis properties with a threshold ratio of saturation remanence to saturation magnetization (M_r/M_s) at 0.22. To obtain reliable Thellier paleointensities on volcanic rocks, rapidly cooled clinkers and scoriae are to be collected, screened for the hysteresis properties, and then heated according to the temperature steps assigned to each sample.

Keywords Paleointensity, Thellier method, Magnetic hysteresis, Curie temperature

*Correspondence:
Koji Fukuma
kfukuma@mail.doshisha.ac.jp
Full list of author information is available at the end of the article

Graphical abstract

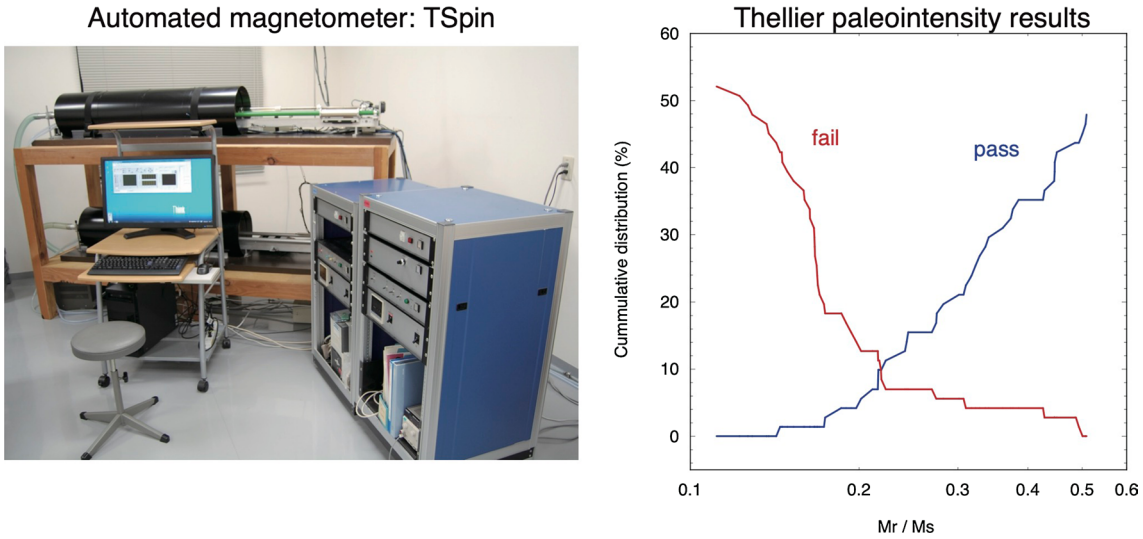

Introduction

The geomagnetic field intensity in the historical or geological past is of prime importance in revealing the evolution of the geomagnetic field itself and its shielding effect against solar wind and cosmic rays (e.g., Livermore et al. 2014; Simon et al. 2016). Thellier measurements (Thellier and Thellier 1959) on fired archaeological artifacts have provided reliable geomagnetic field intensity variations on centennial to millennial timescales (e.g., Brown et al. 2021). To obtain absolute geomagnetic field intensity further in the past, we need to measure igneous rocks, but the success rate of the Thellier method for igneous rocks is substantially worse than that for archaeological artifacts (e.g., Dunlop 2011). A number of alternative methods, including multispecimen (Dekkers and Böhnel 2006), microwave (Hill and Shaw 1999), Tsunakawa–Shaw (Tsunakawa and Shaw 1994), Triaxe (Le Goff and Gallet 2004) methods, and new protocols of the Thellier method (e.g., IZZI protocol, repeating in-field (I) and zero-field (Z) steps alternately (Tauxe and Staudigel 2004; Yu et al. 2004)) have been proposed, but there is still no consensus on which method is appropriate for determining paleointensities of igneous rocks. Selection criteria have become increasingly stringent to avoid anomalous paleointensities, which has led to a decrease in the success rate of Thellier measurements (Jeong et al. 2021).

In addition to improving methods and selection criteria for determining paleointensity, it is also critical to select suitable samples for paleointensity measurements. Igneous rocks generally contain magnetic minerals of various types and grain sizes. In subaerial basalts and andesites, which are most commonly used for paleointensity studies, there are variations in titanomagnetite composition, grain size, and microstructure, and even multiple phases of magnetic minerals may be present in a single sample (Grommé et al. 1969). Vertical variations of paleointensity within a single lava flow, along with magnetic properties, have been investigated on Holocene (Morales et al. 2006), historical (de Groot et al. 2014) or recent (Herrero-Bervera and Valet 2009) lavas. These studies showed that there are considerable variations in Curie temperature and hysteresis properties within a single lava flow, and that reliable paleointensities can be obtained using the Thellier method at some limited vertical intervals. Cromwell et al. (2015) retrieved the expected paleointensities using the Thellier method from glassy materials (pahoehoe ropes and aa spires) of historical or recent Hawaiian lavas.

Testing Thellier paleointensity measurements were performed for vertical sections of thin (0.8—1.5 m thick) basaltic lava flows and scoriae that erupted in 1962 and 1983 in Miyakejima volcanic island, Japan. Preliminary paleointensity studies were conducted on four block samples from the 1983 lava flow (Ueno and Zheng 2011, 2012). This study aims to investigate which parts of the subaerial basalts should be collected and what kinds of magnetic properties are useful for sample selection to obtain reliable paleointensities. Although scoriae have been used in paleointensity experiments (Cromwell and Zhang 2021), this is probably the first time the Thellier method has been applied to recently erupted scoriae of known age. Thellier measurements on igneous rocks

generally result in low success rates despite the need for laborious repetition of heating–cooling cycles, therefore a large number of specimens are heated at a same temperature using a large furnace. However, the composition and grain size of titanomagnetite, i.e., the unblocking temperature distribution, are variable among individual samples. Using a fully automated magnetometer with thermal demagnetizer TSpin (Fukuma and Kono 2016; Kono et al. 1991), we can perform Thellier measurements unattended throughout day and night, but also can set appropriate temperature steps for each sample to improve the success rate.

Sampling and methods

Miyakejima is an active volcanic island located about 200 km south of Tokyo. In 1962 and 1983, fissure eruptions occurred on the mountain flanks, erupting scoriae and then discharging andesitic basalt lava flows down along the valleys to the coast (Tsukui et al. 2005). Both eruptions were short-lived, lasting either 1.5 days in 1962 or 15 h in 1983. Drill cores or block samples were collected at three sites from the 1983 lava flow, one site from the 1983 scoria, and one site each from the 1962 lava flow and the 1962 scoria (Additional file 1: Fig. S1, Table 1). The lava flows were sampled vertically from the lower clinker through the lava interior to the upper clinker, and their vertical positions were measured with respect to the boundary of the lava interior and the lower clinker. We visited the sampling sites several times in May and November 2011 and March 2012. The reason for this is to consider which lithology to collect based on the rock magnetic data obtained in the laboratory. While the solid lava interiors were drilled, the upper and lower clinkers and the scoriae were difficult to drill so that block samples were taken. Drill cores and block samples were oriented using a magnetic compass, but for clinkers some block samples could not be oriented due to spatial constraints.

Prior to Thellier measurements, thermomagnetic analyses and hysteresis measurements were performed on all samples using unweathered rock fragments. Thermomagnetic curves were obtained in Ar gas with a 0.3 T magnetic field using a custom-built semi-horizontal Curie balance (Natsuhara Giken NMB-2000). The Curie temperatures were determined graphically using the two-tangent method for heating curves (Grommé et al. 1969). Hysteresis measurements were made using a vibrating sample magnetometer (Princeton Measurement Corporation MicroMag 3900) by applying ±1 T. Since some samples did not saturate below 1 T, the saturation magnetization values were calculated following the approach to saturation analysis (Fabian 2006) to avoid underestimation of saturation magnetization by conventional

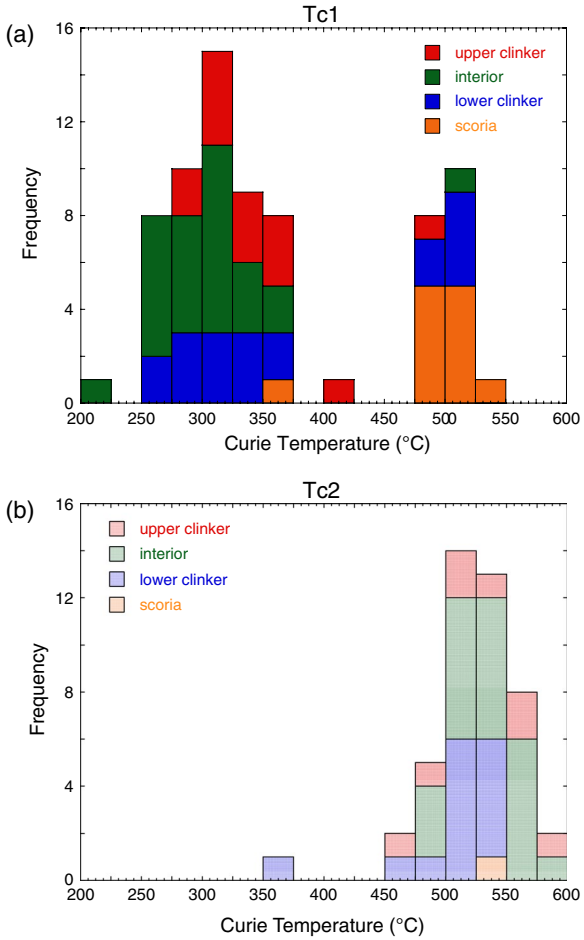

Fig. 1 Histograms of a the lowest Curie temperatures T_{c1} and b the second lowest Curie temperatures T_{c2}. 63% of the samples showed multiple Curie temperatures during thermomagnetic analysis

linear fitting at 0.7−1.0 T. For some selected samples, polished sections were prepared to observe iron–titanium oxides under a digital microscope Keyence VHX-500.

Thellier measurements to obtain paleointensities were performed in air using a fully automated three-component spinner magnetometer with thermal demagnetizer TSpin, which allows unattended overnight measurements (Fukuma and Kono 2016; Kono et al. 1991). In contrast to the usual batch heating, TSpin allows to set up appropriate temperature steps for each sample. Temperature steps were assigned based on the individual thermomagnetic curves, and partial thermoremanent magnetization (pTRM) checks were applied every two temperature steps. Because TSpin places a single sample in exactly the same position in the furnace, temperature variation within the furnace does not affect temperature reproducibility between zero-, in-field, and pTRM check steps. The laboratory magnetic field was set to 45 μT, considering the 1962 and 1983 geomagnetic field intensity in

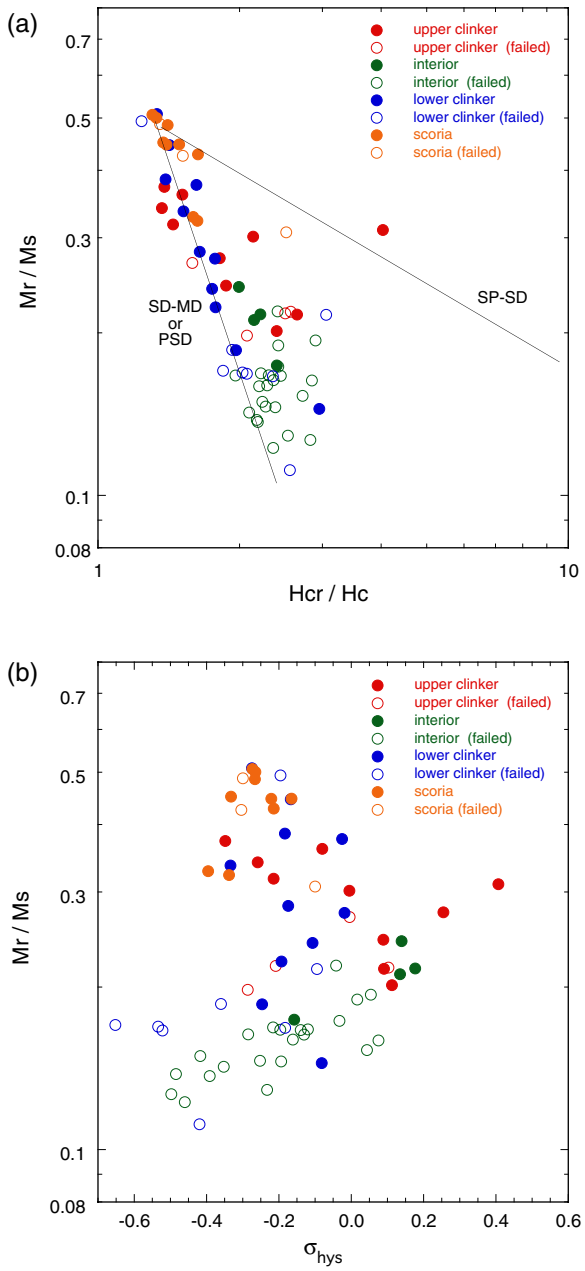

Fig. 2 Hysteresis parameters plotted on a a logarithmic Day plot and b a σ_{hys} (Fabian 2003) plotted against M_r/M_s. The colors represent the different lithologies. The solid and open symbols indicate the passed and failed samples for Thellier measurements, respectively

Miyakejima 45.2 μT and 45.1 μT, respectively, calculated by the International Geomagnetic Reference Field (IGRF) model (Alken et al. 2021).

In order to assess the contribution of multidomain grains through the curvature k on the Arai diagram (Paterson 2011; Paterson et al. 2014), the Coe version (Coe 1967) of the Thellier method, in which a zero-field step precedes an in-field step at a same temperature, was adopted rather than the IZZI protocol (Tauxe and Staudigel 2004; Yu et al. 2004), which yields curved zigzag segments for multidomain grains. In addition to the $|k| < 0.164$ criterion, segments for determining paleointensity were discriminated according to the commonly used criteria of TTA (Leonhardt et al. 2004), PICRIT03 (Kissel and Laj 2004), and SELCRIT2 (Biggin et al. 2007) as modified by Paterson et al. (2014). The remanent magnetizations at the zero-field steps during the Thellier measurement were plotted on a Zijderveld diagram, and the directions of the characteristic remanent magnetization (ChRM) were obtained by principal component analysis (Kirschvink 1980).

Results

Thermomagnetic and hysteresis measurements

Curie temperatures were determined by thermomagnetic analysis to identify magnetic minerals and to confirm thermal stability of the magnetic minerals. Single Curie temperatures were obtained for 37% of the samples, while the remaining 63% had multiple Curie temperatures and two samples exhibited three Curie temperatures (Additional file 1: Table S1). Figure 1 shows the Curie temperatures in histograms by 25°C intervals. The lowest Curie temperature T_{c1} of each sample, which is most prominent in most samples, shows a bimodal distribution with peaks at 300-325°C and 500-525°C intervals, while the second Curie temperature T_{c2} has a single peak at 500-525°C. With respect to the ulvöspinel content (x) of titanomagnetite (Lattard et al. 2006), the median x of the T_{c1} peaks are 0.4 and 0.1, and the T_{c2} peak corresponds to $x = 0.1$. The upper clinkers and the lava interiors are dominated by low T_{c1} titanomagnetite, i.e., Ti-rich titanomagnetite (Fig. 1a, Additional file 1: Fig. S2a, b), and 85% of the lava interiors and 57% of the upper clinkers contain coexisting Ti-poor titanomagnetite (Fig. 1b). The lower clinkers contain coexisting Ti-rich and -poor titanomagnetites or a single phase of Ti-poor titanomagnetite (Additional file 1: Fig. S2c), and the scoriae contain a single phase of Ti-poor titanomagnetite except for one sample (Additional file 1: Fig. S2d). The heating and cooling curves are not significantly different, indicating that titanomagnetite is stable to heating up to 700°C regardless of titanomagnetite composition (Additional file 1: Fig. S2). Although the reversible thermomagnetic curves indicate that the lava flows and scoriae have the potential to yield reliable paleointensities by Thellier measurements, the wide distribution of Curie points suggests that the temperature steps of the Thellier measurements need to be varied for individual samples.

Magnetic hysteresis properties allow us to estimate the grain size of magnetic minerals and explore the possibility of obtaining paleointensities by the Thellier method. Although the composition of titanomagnetite varies (Fig. 1), the Day plot allows the grain size of magnetic minerals to be estimated regardless of the composition of titanomagnetite (Dunlop 2002). The hysteresis parameters were plotted on a logarithmic Day plot as marked differently by lithology (Fig. 2a). Some lower clinker and scoria samples have ratios of saturation remanence over saturation magnetization (M_r/M_s) close to 0.5, suggesting of single-domain grains dominated by shape anisotropy. Since M_r/M_s hardly exceeds 0.5, reliable M_s should be obtained by the approach to saturation analysis (Fabian 2006). While M_r/M_s of 0.2–0.4 in the upper clinker are indicative of relatively fine grains, M_r/M_s in most of the lava interior samples are less than 0.2, indicating that the lava interior is coarsest-grained in the four kinds of lithologies. Hysteresis loops are shown for the same four samples whose thermomagnetic curves are shown in Additional file 1: Fig. S2. The lower clinker (Additional file 1: Fig. S3c) and scoria (Additional file 1: Fig. S3d) exhibit wider loops, the upper clinker loops are narrower (Additional file 1: Fig. S3a), and the lava interior has even narrower loops (Additional file 1: Fig. S3b). To quantify the hysteresis shape, σ_{hys} was calculated and plotted against M_r/M_s (Fig. 2b) (Fabian 2003). Samples with positive σ_{hys} representing constricted (wasp-waisted) shape are limited to a few upper clinker and lava interior samples. Despite the coexistence of Ti-rich and -poor titanomagnetites in many samples (Fig. 1), few samples contain significantly contrasting coercivity components that represent constricted shapes.

Using a digital microscope, polished sections of the upper clinker, the lava interior, and the lower clinker, whose thermomagnetic curves and hysteresis loops are shown in Additional file 1: Figs. S2 and S3, were observed in reflected light (Additional file 1: Fig. S4). The scoriae were too porous and fragile to prepare polished sections by myself. Under the microscope, iron–titanium oxides with high reflectivity could be easily distinguished from the surrounding silicates. None of the samples contained phenocrysts of iron–titanium oxides larger than a few tens of microns. Submicron iron–titanium oxides are abundant and dispersed in the rock matrix in the upper and lower clinkers (Additional file 1: Figs. S4a, c). On the other hand, numerous coarser iron–titanium oxides of a few to 10 μm were found in the lava interior (Additional file 1: Fig. S4b). These differences in grain size correspond to differences in hysteresis loop width (Additional file 1: Figs. S3a–c) and points on the Day plot (Fig. 2a). The iron–titanium oxides were probably formed when the magma erupted from the fissures or during the cooling process of the lava flows after emplacement. Under the digital microscope, it was not possible to resolve the microstructure (e.g., lamellae) within these submicron- or micron-sized iron–titanium oxides.

Thellier measurements

Thellier measurements were performed with TSpin at temperature steps of 25°C or 50°C up to 580°C, which were assigned based on the thermomagnetic curves. Many temperature steps were set in the temperature range where the unblocking temperature spectrum is expected to peak below the Curie point. The samples that showed linear segments over a wide temperature range from room temperature to the Curie point on the Arai diagrams (Arai 1963) were mostly found in the upper and lower clinkers and scoriae (Fig. 3a, d, e). The points of the pTRM check do not deviate significantly from the linear segments, so thermal alteration during Thellier measurements remains minimal for these samples. For the lava interior, many samples show upward concave, two-segmented or sigmoidal (Fig. 3b) and erratic behavior (Fig. 3c) on the Arai diagrams. In the latter case, even the direction of the remanent magnetization is not stable during the Thellier measurements. The Arai and Zijderveld diagrams of all samples are available online together with the thermomagnetic curves and the hysteresis loops, as noted in "Availability of data and materials".

To obtain paleointensities by finding the slope of linear segments on Arai diagrams, several sets of commonly used selection criteria TTA, PICRIT03, and SELCRIT2 modified by Paterson et al. (2014) were used in addition to the curvature criterion $|k| < 0.164$. For a total of 71 samples, the number of passed samples are 34, 21, and 43 for modified TTA, PICRIT03, and SELCRIT2 plus $|k|$ criteria, respectively (Additional file 1: Table S2). PICRIT03 reduced the passed samples due to the criterion of the number of pTRM check points, whereas SELCRIT2 lacks a criterion to examine the cumulative effect of pTRM check and passed many samples. There is still no consensus on which set of criteria should be used to determine paleointensities, but too stringent criteria can reject meaningful results, while too loose criteria introduce errors. Because the TTA criterion has the advantage of using a vector-based parameter when

(See figure on next page.)

Fig. 3 Thellier results plotted on Arai and Zijderveld (insets) diagrams for a upper clinker; b, c lava interior; d lower clinker, and e scoria. In both Arai and Zijderveld diagrams, lines were fitted according to modified TTA and curvature criteria (Leonhardt et al. 2004; Paterson et al. 2014). In Arai diagrams, numbers denote temperatures in °C and open squares indicate partial thermoremanent magnetization checks. Zijderveld diagrams are shown in the sample coordinate projected onto the x-y (blue) and x-z (red) planes

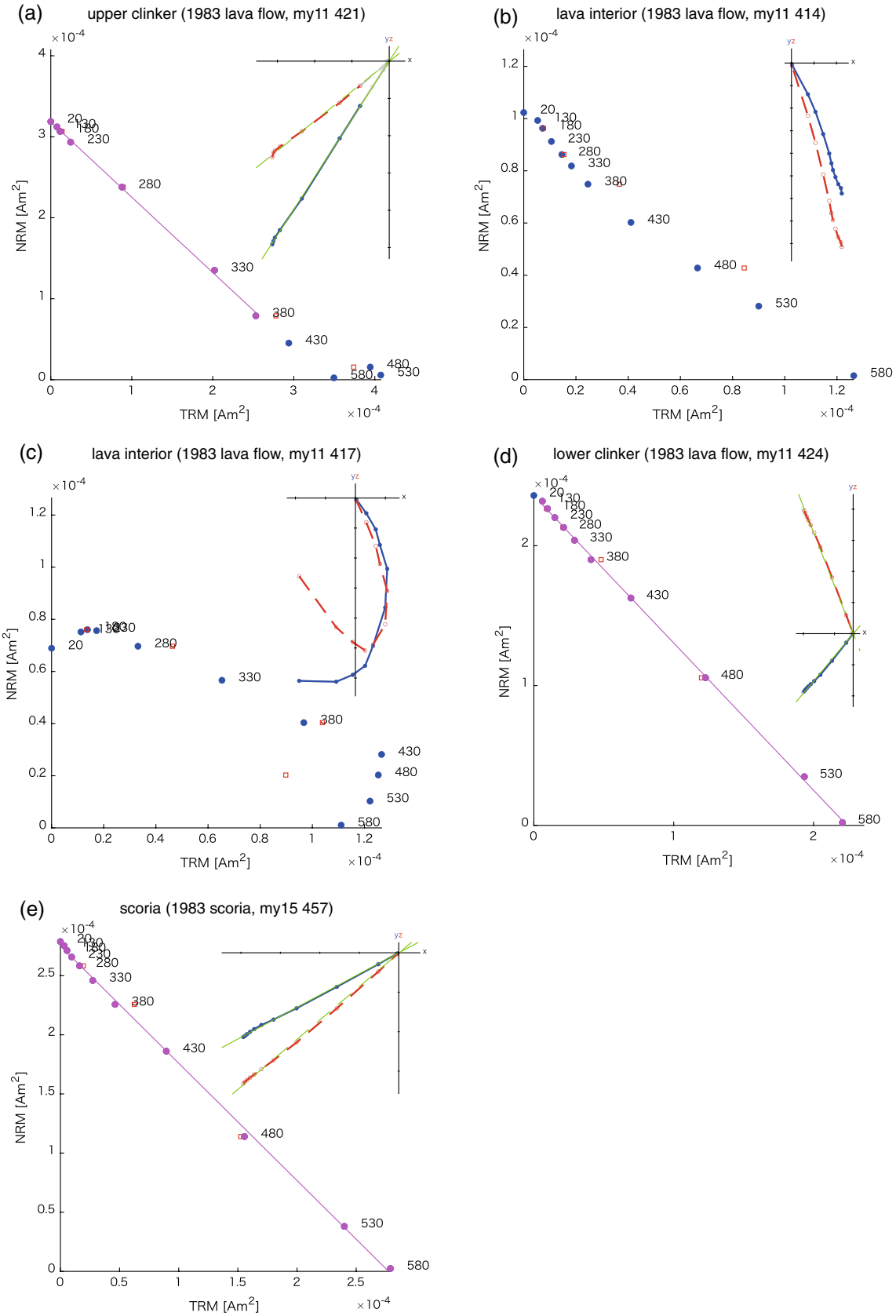

Fig. 3 (See legend on previous page.)

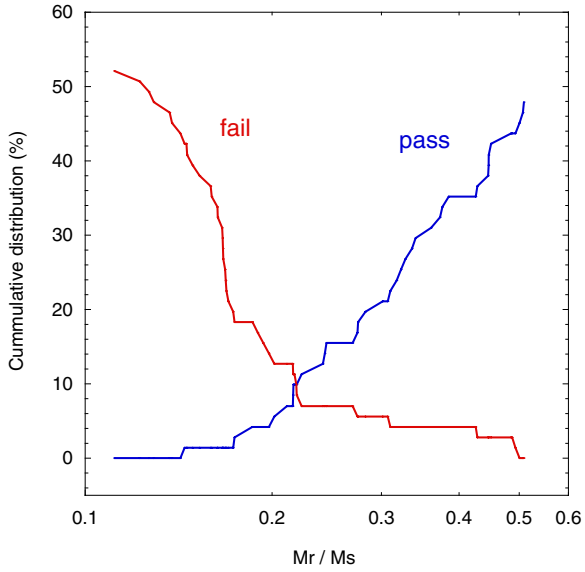

Fig. 4 Cumulative plots of pass and fail rates of Thellier measurements based on TTA and curvature criteria (Leonhardt et al. 2004; Paterson et al. 2014) against M_r/M_s

examining the cumulative effect of the pTRM check, linear segments were evaluated according to the modified TTA and $|k|$.

The pass rates are summarized for each site in Table 1, divided into the upper and lower clinkers and the lava interior in the case of lava flows. The clinkers have much higher pass rates than the lava interior for the four lava flow sites, and the pass rates are also high for the two scoria sites. The pass rate for all samples is 34/71=47.9%, but the pass rate for clinkers and scoriae is 30/45=66.7% and that for the lava interior is 4/26=15.4%, showing a large difference. Pass or fail results related to lithology and hysteresis properties are clearly visible in the Day and σ_{hys}-M_r/M_s plots (Fig. 2), and hence are closely related to grain size. Plotting the cumulative pass and fail rates against M_r/M_s, they intersect at $M_r/M_s \sim 0.22$ (Fig. 4).

For all six sites where four or more samples per site were averaged, the unweighted site means of paleointensity are not significantly different from the expected field intensity of 45.2 μT at 1962 or 45.1 μT at 1983 (Table 1). The standard deviations meet the criteria of less than 5 μT and 10% of the means (Cromwell et al. 2015) except for one site my12 of 1962. The mean of the four 1983 sites is 46.6±3.3 μT, 3.3% greater than the expected value. The single site of 1962 is 4.9% less than the expected value.

To determine ChRM directions at zero-field steps, the fitting ranges on the Zijderveld diagrams were chosen independently of the linear segment range on the Arai diagrams used to derive paleointensities. Therefore, many samples in lava interiors, where paleointensities could not be obtained, yielded ChRMs (Additional file 1: Table S2). By averaging the ChRM directions for each site regardless of lithology, the mean directions and 95% confidence limits are plotted on an equal-area projection along with the 1962 and 1983 geomagnetic field directions at Miyakejima calculated by the IGRF model (Additional file 1: Fig. S5). The declinations vary by several degrees because the azimuths were measured with a magnetic compass, and the inclinations are a few degrees shallower than the expected, as often reported for historical lavas (e.g., Pavón-Carrasco et al. 2016). Nevertheless, all six sites do not yield ChRMs that deviated much from 1962 and 1983 field directions, suggesting that the upper and lower clinkers and scoriae acquired remanent magnetizations after emplacement, as did the lava interior.

Table 1 Summary of Thellier paleointensity results for 1962 and 1983 lava flows and scoriae in Miyakejima, Japan

Age	Material	Site	lat.(°N)	lon.(°E)	Pass rate		B_a (μT)	σ(%)	Δ(%)
					Clinker or scoria	Lava interior			
1983	Lava flow	my07	34.074453	139.508991	9/12	0/10	49.1 ± 4.7	9.6	
1983	Lava flow	my11	34.060768	139.499107	6/9	0/4	47.9 ± 4.7	9.8	
1983	Lava flow	my10	34.051535	139.492885	4/8	1/4	41.8 ± 4.1	9.9	
1983	Scoria	my15	34.062000	139.482678	4/6	—	47.7 ± 2.2	4.6	
1983							46.6 ± 3.3		+3.3
1962	Lava flow	my03	34.096662	139.563913	2/4	3/8	43.0 ± 4.0	9.3	
1962	Scoria	my12	34.096764	139.559096	5/6	—	42.7 ± 5.8	13.5	
1962							43.0		−4.9
total					30/45	4/26			

Pass rates are based on modified TTA and curvature criteria (Leonhardt et al. 2004; Paterson et al. 2014). B_a, σ and Δ denote paleointensity averages ± standard deviations, standard deviations in percent for each site, and differences from expected field intensities in percent for 1983 and 1962, respectively. The expected field intensities of 1962 and 1983 are 45.2 and 45.1 μT, respectively

Discussion

For subaerial basalts and andesites, paleomagnetic samples have usually been collected by drilling from solidified lava interiors. This is because lava interiors are easy to drill and drill cores are more accurately oriented than block samples (Turner et al. 2015). Not only are the upper and lower clinkers and scoriae difficult to drill, but there has also been concern that the clinkers and scoriae may have moved and tilted after acquiring natural remanent magnetization (NRM). However, as can be seen in the ChRM directions (Fig. S5), they do not appear to have suffered significant tilting (Additional file 1: Table S2). On the other hand, slowly cooled lava interiors are more likely to acquire chemical or thermochemical remanent magnetization and develop microstructures such as lamellae within a titanomagnetite grain.

Linearity between the NRM of TRM origin and the TRM imparted in the laboratory, a prerequisite for the Thellier method, requires that the sample contain single-domain or pseudo-single-domain grains that must be retained during laboratory heating (Dunlop 2011). Lamellae may result in fine-grained (Dunlop and Özdemir 2015), but thermal instability of the microstructure leads to failure of Thellier measurements (Tanaka and Yamamoto 2016). Also the lavas with intermediate high temperature oxidation state give erroneously high Thellier paleointensities (Mochizuki et al. 2004; Oishi et al. 2005; Yamamoto et al. 2003). Samples from lava interiors are likely to violate the prerequisite of the Thellier method, and the low pass rate of 15.4% in the present Thellier measurements indicates that lava interiors are not suitable for paleointensity determination. Even if block samples are not so accurately oriented or left unoriented, the upper and lower clinkers and scoriae, which are rapidly cooled, fine-grained, and dominated by a single phase of titanomagnetite, are worth collecting for Thellier measurements. Glassy materials, such as pahoehoe ropes and aa spires, provided accurate Thellier paleointensities (Cromwell et al. 2015), but are easily weathered and eroded (Cromwell et al. 2018). Upper clinkers and scoriae are also susceptible to erosion, but lower clinkers are covered by the overlying lava and are difficult to erode. I recovered fresh dark gray specimens under the rough and reddish surface of the lower clinkers.

The Thellier method works well for fired archaeological artifacts because fine-grained, nearly pure magnetites in many cases carry their remanent magnetization. In contrast, lava flows and scoriae have wide distributions of titanomagnetite composition and grain size, which are variable even within a single lava flow (e.g., de Groot et al. 2014). It is desirable to estimate the unblocking temperature distribution before performing Thellier measurements, and to set appropriate temperature steps for each sample. To avoid obtaining erroneous paleointensity by fitting a segment with a few points on an Arai diagram, commonly used selection criteria include parameters that limit the minimum number of points to be fitted and the spacing between points (Paterson et al. 2014). When heating multiple samples in a single batch, it is often the case that many points fall outside the unblocking temperature range and these parameters are not met. With TSpin, the measurement and heating is performed on one specimen at a time, allowing the temperature steps to be set for each specimen based on the thermomagnetic curve. The titanomagnetite composition of the present sample set shows a bimodal distribution with x centered at 0.1 and 0.4 (Fig. 1), but the non-uniform composition distribution was absorbed by the flexible setting of temperature steps for each sample. The reason that the Thellier method has not been very successful with igneous rocks may be partly due to the batch heating that is often used.

Although the temperature settings of the Thellier method can accommodate differences in titanomagnetite composition, for grain size the only option is to choose samples with single-domain-like properties. Measuring clinker and scoria samples is itself a rough screening by grain size, but lithological change in a lava flow is gradual. As shown in Fig. 2, pass and fail sample points are placed in distinctly different areas on the Day and σ_{hys}-M_r/M_s plots. The cumulative distribution of pass and fail to the TTA and curvature criteria against M_r/M_s shows that the number of pass samples increases linearly for log-scale M_r/M_s from about 0.2 up to 0.5, while for $M_r/M_s < 0.2$ most samples fail Thellier measurements. Similarly Di Chiara et al. (2017) found a threshold of $M_r/M_s < 0.2$ for Paleoproterozoic mafic sills, and Calvo et al. (2002) reported the failure of all Thellier experiments for historical lava flows with $M_r/M_s < 0.2$ regardless of the magnetic minerals contained. Conversely, Carvallo et al. (2006) noted that for a large sample collection of igneous rocks, hysteresis properties do not appear to correlate with the success or failure of Thellier measurements. Thermal alteration as well as grain size can have a significant influence on Thellier results of the sample collection, which includes geological samples of various ages. Here, Thellier measurements on thermally stable recent basalts, where the true field strength is known, allow us to clearly see the effect of domain state on success or failure. Past geomagnetic field intensity could be efficiently obtained by measuring rapidly cooled samples that were screened with $M_r/M_s > 0.2$.

The Thellier method was originally developed to retrieve past geomagnetic field intensities from fired archaeological artifacts (Thellier and Thellier 1959). Since its development, about 90% of the archeointensities have been produced by the Thellier method (Brown et al. 2021). The Thellier method in its current form is more advanced; pTRM check (Coe 1967) for thermal alteration, and tail check (Riisager and Riisager 2001), IZZI protocol (Tauxe and Staudigel 2004; Yu et al. 2004), or curvature criteria (Paterson 2011) for multidomain effect are built-in. Various alternative paleointensity methods have been devised, but none has yet replaced the Thellier method. There will never be available a single paleointensity method applicable to all igneous rocks, which contain magnetic minerals with a wide variety in composition and grain size. A realistic best practice would be to search for certain kinds of igneous rocks that contain thermally stable single-domain-like grains, similar to many fired archaeological artifacts. The clinkers and scoriae of subaerial basalts presented here are just examples.

Conclusions

Reliable Thellier paleointensities were obtained at all six sites of the 1962 and 1983 lava flows and scoriae of Miyakejima Volcano, and the paleointensities at 1962 and 1983 are within 5% of the expected values. Rapidly cooled upper and lower clinkers and scoriae show a pass rate of 66.7% of the Thellier results for TTA and curvature criteria, which is 4.3 times higher than that of the lava interior. The high pass rate of the clinkers and scoriae is consistent with the predominance of single-phase titanomagnetite, either Ti-rich ($x \sim 0.4$) or Ti-poor ($x \sim 0.1$), and with the fine-grained assemblages. For Thellier measurements using TSpin, the criteria were better met by assigning different temperature steps to each sample according to titanomagnetite composition. In terms of grain size, the threshold M_r/M_s is 0.22, where the cumulative pass rate exceeds the cumulative fail rate. The Thellier method on volcanic rocks, mainly on lava interiors, has so far shown significantly lower pass rates than fired archaeological artifacts, leading to the development of various alternative paleointensity methods. However, when block samples of clinker and scoria are collected, then screened for M_r/M_s, and individually temperature steps are set on the basis of thermomagnetic curves, the Thellier method yields reliable paleointensities with a high pass rate comparable to that of fired archaeological artifacts. Weathering-resistant rapidly cooled igneous rocks, such as lower clinkers, will provide us with reliable past variations of geomagnetic field intensity beyond archeological time.

Supplementary Information

The online version contains supplementary material available at https://doi.org/10.1186/s40623-023-01781-z.

Additional file 1: Figure S1. Sampling sites of 1962 and 1983 lava flows (L) and scoria (S) in Miyakejima, Japan. **Figure S2.** Thermomagnetic curves for (a) the upper clinker, (b) the lava interior, and (c) the lower clinker of the 1983 lava flow at site my11, and (d) the 1983 scoria at site my15. Heating and cooling curves are shown as red and blue curves, respectively. **Figure S3.** Hysteresis loops for (a) the upper clinker, (b) the lava interior, and (c) the lower clinker of the 1983 lava flow at site my11, and (d) the 1983 scoria at site my15. **Figure S4.** Microscope photographs for (a) the upper clinker, (b) the lava interior, and (c) the lower clinker of the 1983 lava flow at site my11. Each white scale bar indicates 100 µm. **Figure S5.** Site mean directions with their 95% confidence limits of characteristic remanent magnetizations deduced from zero-field steps of Thellier measurements plotted on an equal-area projection. Red open symbols indicate the 1962 and 1983 geomagnetic field directions in Miyakejima, Japan, derived from the IGRF model (Alken et al. 2021). **Table S1.** Curie temperatures and hysteresis parameters for 1962 and 1983 lava flows and scorias in Miyakejima, Japan. **Table S2.** Thellier paleointensity results for 1962 and 1983 lava flows and scorias in Miyakejima, Japan.

Acknowledgements

The author is grateful to Masahiro Ooga for his assistance in sampling and Minoru Kawamura for carefully preparing samples. The author would also like to thank Hyeon-Seon Ahn and an anonymous reviewer for their careful and constructive reviews, and the handling editor, Nobutatsu Mochizuki.

Author contributions

The author maintained TSpin, performed sampling, measurements and data analysis, and drafted the manuscript. The author read and approved the final version of the manuscript.

Funding

This work was supported by a Grant-in-Aid for Scientific Research (19K04020).

Availability of data and materials

Thermomagnetic curves, hysteresis loops, and Arai and Zijderveld diagrams of the Thellier results are available at https://doi.org/10.5281/zenodo.6922806 and the raw data are also available from the author upon reasonable request. The datasets of Additional file 1:Table S1 and Table S2 are available at https://doi.org/10.5281/zenodo.6922877.

Declarations

Competing interests

The author declares that he has no competing interests.

Author details

[1]Department of Environmental System Science, Doshisha University, Kyotanabe 610-0394, Japan.

Received: 29 July 2022 Accepted: 29 January 2023
Published online: 24 February 2023

References

Alken P, Thébault E, Beggan CD, Amit H, Aubert J, Baerenzung J, Bondar TN, Brown WJ, Califf S, Chambodut A, Chulliat A, Cox GA, Finlay CC, Fournier A, Gillet N, Grayver A, Hammer MD, Holschneider M, Huder L, Hulot G, Jager T, Kloss C, Korte M, Kuang W, Kuvshinov A, Langlais B, Léger JM, Lesur V, Livermore PW, Lowes FJ, Macmillan S, Magnes W, Mandea M, Marsal S, Matzka J, Metman MC, Minami T, Morschhauser A, Mound

JE, Nair M, Nakano S, Olsen N, Pavón-Carrasco FJ, Petrov VG, Ropp G, Rother M, Sabaka TJ, Sanchez S, Saturnino D, Schnepf NR, Shen X, Stolle C, Tangborn A, Tøffner-Clausen L, Toh H, Torta JM, Varner J, Vervelidou F, Vigneron P, Wardinski I, Wicht J, Woods A, Yang Y, Zeren Z, Zhou B (2021) International Geomagnetic Reference Field: the thirteenth generation. Earth Planets Space 73:49. https://doi.org/10.1186/s40623-020-01288-x

Arai Y (1963) Secular variation in the intensity of the past geomagnetic field. M. Sc. Thesis, Univ. Tokyo 84

Biggin AJ, Perrin M, Dekkers MJ (2007) A reliable absolute palaeointensity determination obtained from a non-ideal recorder. Earth Planetary Sci Lett 257:545–563. https://doi.org/10.1016/j.epsl.2007.03.017

Brown MC, Hervé G, Korte M, Genevey A (2021) Global archaeomagnetic data: The state of the art and future challenges. Phys Earth Planet Inter 318:106766. https://doi.org/10.1016/j.pepi.2021.106766

Calvo M, Prévot M, Perrin M, Riisager J (2002) Investigating the reasons for the failure of palaeointensity experiments: a study on historical lava flows from Mt. Etna (Italy). Geophys J Int 149:44–63. https://doi.org/10.1046/j.1365-246X.2002.01619.x

Carvallo C, Roberts AP, Leonhardt R, Laj C, Kissel C, Perrin M, Camps P (2006) Increasing the efficiency of paleointensity analyses by selection of samples using first-order reversal curve diagrams. J Geophys Res Solid Earth 111:B12103. https://doi.org/10.1029/2005JB004126

Coe RS (1967) Paleointensities of the Earth's magnetic field determined from Tertiary and Quaternary rocks. J Geophys Res 72:3247–3262. https://doi.org/10.1029/JZ072i012p03247

Cromwell G, Tauxe L, Staudigel H, Ron H (2015) Paleointensity estimates from historic and modern Hawaiian lava flows using glassy basalt as a primary source material. Phys Earth Planet Inter 241:44–56. https://doi.org/10.1016/j.pepi.2014.12.007

Cromwell G, Trusdell F, Tauxe L, Staudigel H, Ron H (2018) Holocene paleointensity of the Island of Hawai 'i from glassy volcanics. Geochem Geophys Geosys 19:3224–3245. https://doi.org/10.1002/2017GC006927

Cromwell G, Zhang Y (2021) New paleointensity data from Aniakchak Volcano. Geochemistry, Geophysics, Geosystems, Alaska, USA. https://doi.org/10.1029/2021GC010032

Dekkers MJ, Böhnel HN (2006) Reliable absolute palaeointensities independent of magnetic domain state. Earth Planet Sci Lett 248:508–517. https://doi.org/10.1016/j.epsl.2006.05.040

Di Chiara A, Muxworthy AR, Trindade RIF, Bispo-Santos F (2017) Paleoproterozoic geomagnetic field strength from the Avanavero mafic sills, Amazonian Craton, Brazil. Geochem Geophys Geosys 18:3891–3903. https://doi.org/10.1002/2017GC007175

Dunlop D, Özdemir Ö (2015) Magnetizations in Rocks and Minerals. In: Schubert G (ed) Treatise on Geophysics. Elsevier, Oxford

Dunlop DJ (2002) Theory and application of the Day plot (Mrs/Ms versus Hcr/Hc) 1Theoretical curves and tests using titanomagnetite data. J Geophys Res Solid Earth. https://doi.org/10.1029/2001JB000486

Dunlop DJ (2011) Physical basis of the Thellier-Thellier and related paleointensity methods. Phys Earth Planet Inter 187:118–138. https://doi.org/10.1016/j.pepi.2011.03.006

Fabian K (2003) Some additional parameters to estimate domain state from isothermal magnetization measurements. Earth Planet Sci Lett 213:337–345. https://doi.org/10.1016/S0012-821X(03)00329-7

Fabian K (2006) Approach to saturation analysis of hysteresis measurements in rock magnetism and evidence for stress dominated magnetic anisotropy in young mid-ocean ridge basalt. Phys Earth Planet Inter 154:299–307. https://doi.org/10.1016/j.pepi.2005.06.016

Fukuma K, Kono M (2016) A LabVIEW software for Thellier paleointensity measurements with an automated three-component spinner magnetometer TSpin. Earth Planets Space 68:43. https://doi.org/10.1186/s40623-016-0424-2

Grommé CS, Wright TL, Peck DL (1969) Magnetic properties and oxidation of iron-titanium oxide minerals in alae and makaopuhi lava lakes, hawaii. J Geophys Res 74:5277–5293. https://doi.org/10.1029/JB074i022p05277

de Groot LV, Dekkers MJ, Visscher M, ter Maat GW (2014) Magnetic properties and paleointensities as function of depth in a Hawaiian lava flow. Geochem Geophys Geosys 15:1096–1112. https://doi.org/10.1002/2013GC005094

Herrero-Bervera E, Valet JP (2009) Testing determinations of absolute paleointensity from the 1955 and 1960 Hawaiian flows. Earth Planet Sci Lett 287:420–433. https://doi.org/10.1016/j.epsl.2009.08.035

Hill MJ, Shaw J (1999) Palaeointensity results for historic lavas from Mt Etna using microwave demagnetization/remagnetization in a modified Thellier-type experiment. Geophys J Int 139:583–590. https://doi.org/10.1046/j.1365-246x.1999.00980.x

Jeong D, Liu Q, Yamamoto Y, Yu Y, Zhao X, Qin H (2021) New criteria for selecting reliable Thellier-type paleointensity results from the 1960 Kilauea lava flows. Hawaii Earth Planets Space 73:144. https://doi.org/10.1186/s40623-021-01473-6

Kirschvink JL (1980) The least-squares line and plane and the analysis of palaeomagnetic data. Geophys J Royal Astron Soc 62:699–718. https://doi.org/10.1111/j.1365-246X.1980.tb02601.x

Kissel C, Laj C (2004) Improvements in procedure and paleointensity selection criteria (PICRIT-03) for Thellier and Thellier determinations: application to Hawaiian basaltic long cores. Phys Earth Planet Inter 147:155–169. https://doi.org/10.1016/j.pepi.2004.06.010

Kono M, Hoshi M, Yamaguchi K, Nishi Y (1991) An automatic spinner magnetometer with thermal demagnetization equipment. J Geomagn Geoelect 43:429–443. https://doi.org/10.5636/jgg.43.429

Lattard D, Engelmann R, Kontny A, Sauerzapf U (2006) Curie temperatures of synthetic titanomagnetites in the Fe-Ti-O system: Effects of composition, crystal chemistry, and thermomagnetic methods. J Geophys Res Solid Earth. https://doi.org/10.1029/2006JB004591

Le Goff M, Gallet Y (2004) A new three-axis vibrating sample magnetometer for continuous high-temperature magnetization measurements: applications to paleo- and archeo-intensity determinations. Earth Planet Sci Lett 229:31–43. https://doi.org/10.1016/j.epsl.2004.10.025

Leonhardt R, Heunemann C, Krása D (2004) Analyzing absolute paleointensity determinations: acceptance criteria and the software ThellierTool4.0. Geochem Geophys Geosyst 5:Q12016. https://doi.org/10.1029/2004GC000807

Livermore PW, Fournier A, Gallet Y (2014) Core-flow constraints on extreme archeomagnetic intensity changes. Earth Planet Sci Lett 387:145–156. https://doi.org/10.1016/j.epsl.2013.11.020

Mochizuki N, Tsunakawa H, Oishi Y, Wakai S, Wakabayashi K, Yamamoto Y (2004) Palaeointensity study of the Oshima 1986 lava in Japan: implications for the reliability of the Thellier and LTD-DHT Shaw methods. Phys Earth Planet Inter 146:395–416. https://doi.org/10.1016/j.pepi.2004.02.007

Morales J, Alva-Valdivia LM, Goguitchaichvili A, Urrutia-Fucugauchi J (2006) Cooling rate corrected paleointensities from the Xitle lava flow: evaluation of within-site scatter for single spot-reading cooling units. Earth Planets Space 58:1341–1347. https://doi.org/10.1186/BF03352630

Oishi Y, Tsunakawa H, Mochizuki N, Yamamoto Y, Wakabayashi KI, Shibuya H (2005) Validity of the LTD-DHT Shaw and Thellier palaeointensity methods: a case study of the Kilauea 1970 lava. Phys Earth Planet Inter 149:243–257. https://doi.org/10.1016/j.pepi.2004.10.009

Paterson GA (2011) A simple test for the presence of multidomain behavior during paleointensity experiments. J Geophys Res Solid Earth 116:B10104. https://doi.org/10.1029/2011JB008369

Paterson GA, Tauxe L, Biggin AJ, Shaar R, Jonestrask LC (2014) On improving the selection of Thellier-type paleointensity data. Geochem Geophys Geosys 15:1180–1192. https://doi.org/10.1002/2013GC005135

Pavón-Carrasco FJ, Tema E, Osete ML, Lanza R (2016) Statistical analysis of palaeomagnetic data from the last four centuries: Evidence of systematic inclination shallowing in lava flow records. Pure Appl Geophys 173:839–848. https://doi.org/10.1007/s00024-014-0946-0

Riisager P, Riisager J (2001) Detecting multidomain magnetic grains in thellier palaeointensity experiments. Phys Earth Planet Inter 125:111–117. https://doi.org/10.1016/S0031-9201(01)00236-9

Simon Q, Thouveny N, Bourlès DL, Valet JP, Bassinot F, Ménabréaz L, Guillou V, Choy S, Beaufort L (2016) Authigenic 10Be/9Be ratio signatures of the cosmogenic nuclide production linked to geomagnetic dipole moment variation since the Brunhes/Matuyama boundary. J Geophys Res Solid Earth 121:7716–7741. https://doi.org/10.1002/2016JB013335

Tanaka H, Yamamoto Y (2016) Palaeointensities from Pliocene lava sequences in Iceland: emphasis on the problem of Arai plot with two linear segments. Geophys J Int 205:694–714. https://doi.org/10.1093/gji/ggw031

Tauxe L, Staudigel H (2004) Strength of the geomagnetic field in the Cretaceous Normal Superchron: New data from submarine basaltic glass of the Troodos Ophiolite. Geochem Geophys Geosys. https://doi.org/10.1029/2003GC000635

Thellier E, Thellier O (1959) Sur l'intensité du champ magnétique terrestre dans le passé historique et géologique. Ann Geophys 15:285–376
Tsukui M, Kawanabe Y, Niihori K (2005) Geological map of Miyakejima Volcano. Geological Map of Volcanoes No.12, Geological Survey of Japan. https://www.gsj.jp/Map/EN/docs/vol_doc/volcanoe-12.html
Tsunakawa H, Shaw J (1994) The Shaw method of palaeointensity determinations and its application to recent volcanic rocks. Geophys J Int 118:781–787. https://doi.org/10.1111/j.1365-246X.1994.tb03999.x
Turner G, Rasson J, Reeves C (2015) Observation and Measurement Techniques. In: Schubert G (ed) Treatise on Geophysics. Elsevier, Oxford
Ueno N, Zheng Z (2011) Paleointensity determination and rock-magnetic characters of Miyakejima 1983 lava, Japan. J Toyo Univ Nat Sci 55:163–181
Ueno N, Zheng Z (2012) Paleointensity determination of Miyakejima 1983 lava, Japan (2). J Toyo Univ Nat Sci 56:177–215
Yamamoto Y, Tsunakawa H, Shibuya H (2003) Palaeointensity study of the Hawaiian 1960 lava: implications for possible causes of erroneously high intensities. Geophys J Int 153:263–276. https://doi.org/10.1046/j.1365-246X.2003.01909.x
Yu Y, Tauxe L, Genevey A (2004) Toward an optimal geomagnetic field intensity determination technique. Geochem Geophys Geosys. https://doi.org/10.1029/2003GC000630

Publisher's Note